



## RESEARCH ARTICLE

Journal of  
**RAMAN  
SPECTROSCOPY**

WILEY

# Raman spectroscopy of ethane ( $C_2H_6$ ) to 120 GPa at 300 K

Liam Q. Read | James E. Spender | John E. Proctor

Materials and Physics Research Group,  
School of Science, Engineering and  
Environment, University of Salford,  
Manchester, UK

**Correspondence**

John E. Proctor, Materials and Physics  
Research Group, School of Science,  
Engineering and Environment, University  
of Salford, Manchester M5 4WT, UK.  
Email: j.e.proctor@salford.ac.uk

**Abstract**

We have conducted a Raman study of solid ethane ( $C_2H_6$ ) at pressures up to 120 GPa at 300 K. We observe changes within the  $\nu_3$  and  $\nu_{11}$  Raman-active vibrational modes providing evidence for several previously unobserved phase transitions at room temperature. These are located from 16 to 20 GPa, ~35 GPa, and ~60 GPa. We also could no longer measure the  $\nu_3$  and  $\nu_{11}$  modes from 75 GPa onward. We did not, however, observe any signs of the ethane molecule undergoing decomposition, up to the highest pressures measured. We also recorded spectra of the  $(2\nu_8, 2\nu_{11})$ ,  $\nu_1$ , and  $\nu_{10}$  modes but observed more limited changes in the behaviour of these modes.

**KEY WORDS**

diamond anvil, ethane, high pressure, hydrogen, planets

## 1 | INTRODUCTION

Relatively little is known about the behaviour of ethane ( $C_2H_6$ ) at high pressure. The fundamental equation of state (EOS) of the fluid states is backed by experimental data only to 0.07 GPa [1], and we recently published a detailed Raman study of the liquid state at 300 K up to crystallization at 2.5 GPa [2]. As far as the solid phases are concerned, there are two works available covering the pressure range up to ~8 GPa [3, 4], which are in disagreement. All that is available at higher pressure is a single limited set of EOS measurements [5]. To our knowledge, the melting curve above 300 K has not been studied, though decomposition of ethane to hydrogen and diamond has been observed in laser heating experiments in the diamond anvil high-pressure cell (DAC) [6].

This absence of data is surprising in terms of ethane's uniqueness and importance. It is structurally unique, being the simplest molecule with an  $sp^2$  C–C bond. This single C–C bond allows the ethane molecule to rotate its two methyl groups but requires enough energy to overcome the 'ethane barrier' to do so [7]. Understanding

how ethane's structure is affected by high pressures could give insights into the structural behaviour of all single C–C bond molecules, molecules such as ethanol with major technological importance. The C–C bond is in itself the most common foundation of organic molecules.

Ethane itself is a naturally occurring hydrocarbon. It is the second most common component of earth's natural gas deposits behind methane. It is a known constituent of the outer planets as it has been detected in each outer planet's atmosphere [8–10] where it is formed out of methane undergoing photolysis [10]. It holds a notable position within Uranus in particular, as it is suggested that condensation of ethane at the lower stratosphere is partially responsible for Uranus's blue hazed appearance [11]. Understanding ethane's behaviour at high pressure could give strong insights into the internal structures of the gas giants.

Ethane is known to have three solid phases at low temperature, at pressures close to 0.1 MPa: a plastic orientationally disordered Phase I between 90.32 and 89.78 K [12], an orientationally ordered Phase II in a narrow band between 89.78 to 89.68 K [12], and a

This is an open access article under the terms of the Creative Commons Attribution License, which permits use, distribution and reproduction in any medium, provided the original work is properly cited.

© 2020 The Authors. Journal of Raman Spectroscopy published by John Wiley & Sons Ltd

monoclinic Phase III below 89.68 K [13]. At ambient temperature (under high pressure), ethane solidifies at 2.5 GPa. Shimizu et al. [3] proposed (on the basis of Raman measurements) that the ethane crystallized into Phase II, followed by a transition into Phase III upon pressure increase to 3.5 GPa. Later, Podsiadlo et al. [4] proposed (from a single crystal diffraction study using a laboratory x-ray source, at 2.70 and 5.90 GPa) that the ethane instead crystallized into a phase not previously observed in low temperature experiments: Phase IV. Goncharov et al. [5] proposed (from a synchrotron powder x-ray diffraction study) that crystallization at 300 K was to ‘phase A’ (most likely the same phase as Podsiadlo et al.’s Phase IV), followed by a transition to Phase III but not until much higher pressure (18 GPa). The hydrogen atom positions are fixed in Phase III but not in Phase IV—in this phase, rotation of the CH<sub>3</sub> groups is possible. No further transitions were observed up until 120 GPa, the highest pressure reached in this study. However, due to the very limited details given in Goncharov et al. [5] and to the limited information on hydrogen atom positions that can be obtained from an x-ray diffraction experiment in any case, it is not clear whether their data constitute evidence of absence, or just absence of evidence.

The purpose of this paper is to present a study of high-pressure Raman scattering of solid ethane up to 120-GPa pressure. We follow this with an analysis of our spectra to discern if any phase transitions may take place at 300 K under pressures greater than 8 GPa.

## 2 | EXPERIMENTAL

We conducted three different experiments: Experiment 1 covered 10–45 GPa, Experiment 2 covered 75–120 GPa, and Experiment 3 covered both 6–11 and 36–67 GPa.

Pressure was applied using a custom-constructed piston-cylinder DAC. This was fitted with 450-μm diameter diamond culets during Experiment 1, 100-μm diameter bevelled diamond culets during Experiment 2, and 250-μm diameter diamond culets during Experiment 3. A gasket was constructed for each experiment by indenting rhenium foil using the DAC before drilling a hole in the centre of the indent that was approximately 50% the diameter of the diamond culets. The hole was drilled using a custom-constructed spark eroder device. The gasket was then placed onto the piston end diamond culet with a ruby crystal placed within the gasket hole sample space to allow for pressure measurements using the ruby fluorescence method. The DAC was then placed in a small chamber into which gaseous ethane was pumped after being purged of air. The chamber was cooled using

a liquid nitrogen bath causing the condensation of the ethane into its liquid state. Liquid ethane was then allowed to build up until completely submerging the DAC. Pressure was then applied on the collected ethane sample while still submerged to prevent its evaporation. The DAC was then removed, and data collection began.

Raman spectra were then collected with increases in pressure. Raman spectra were measured using a single grating spectrometer, one with a 1,800 lines per mm grating for Experiment 1 and one with a 1,200 lines per mm grating for Experiments 2 and 3. The spectral resolution is 4.8 cm<sup>-1</sup> full width half maximum (FWHM) for Experiment 1 and 6.5 cm<sup>-1</sup> FWHM for Experiments 2 and 3. A 532-nm laser beam with a spot size of ~1 μm provided the light source. For each experiment, an initial spectrum for the Raman peak of silicon was taken to provide calibration between experiments. Pressure was measured using the ruby fluorescence [14] method up to 61 GPa, after which the ruby fluorescence peaks were too weak to measure accurately. Measurement of the pressure-induced shift of the diamond Raman peak was used instead for 62 GPa and above [15]. Both methods were used from 60 to 62 GPa to check for discrepancies between pressure measurement methods, which differed in readings by less than 1 GPa. The ruby fluorescence peak position was determined by fitting Lorentzians. The derivative of the diamond Raman peak was fitted with a Lorentzian to determine diamond measured pressures as described in Akahama and Kawamura [15]. The Raman peaks of ethane were fitted with Lorentzians after background was subtracted to determine position. The error in ruby fluorescence peak position, diamond Raman peak position, and ethane Raman peak position can be estimated by the error in the Lorentzian curve fits. These are typically too small to display.

## 3 | RESULTS

Solid ethane has been described with four first-order Raman active modes at low temperature that we also see at ambient temperature, at high pressure. These are the ν<sub>3</sub> C-C stretching mode, the ν<sub>11</sub> C-H<sub>3</sub> deformation mode, the ν<sub>1</sub> C-H totally symmetric stretching mode, and the ν<sub>10</sub> C-H stretching mode [16]. We are using the nomenclature from our paper on liquid ethane [2]. Further details on the Raman mode assignment are provided in the supporting information.

We will describe the behaviour observed in each Raman mode separately. The lowest wavenumber mode is the ν<sub>3</sub> C-C stretching mode located around 1,030 cm<sup>-1</sup> at 6 GPa. ν<sub>3</sub> is fitted as two distinct components, as has been done in previous studies [3]. The peaks start

$\sim 15 \text{ cm}^{-1}$  apart. At 16 GPa, we observe a splitting of the  $\nu_3(2)$  peak forming a third component of the  $\nu_3$  mode, designated  $\nu_3(3a)$ . Figure 1a shows example spectra of this region up to 25 GPa.

Beyond 25 GPa, the  $\nu_3(3a)$  is not observed. Both remaining  $\nu_3$  components increase roughly linearly in wavenumber against pressure until  $\nu_3(2)$  starts to sharply plateau after 30 GPa. Following this, we once again observe a third component of the  $\nu_3$  mode starting at 36 GPa designated  $\nu_3(3b)$ .  $\nu_3(2)$  then degrades increasingly until disappearing from measurement by 55 GPa. Figure 1b displays examples of this taking place upon increasing pressure.

The  $\nu_3$  mode then experiences a small but discontinuous jump in wavenumber against pressure after passing 60 GPa, following which the  $\nu_3(3b)$  component degrades from measurement by 64 GPa. Example spectra demonstrating this are given in the supporting information. The  $\nu_3$  mode is no longer visible by 75 GPa and is not detected again within our 120 GPa upper bound. A complete picture of collected peak positions is viewable in Figure 2.

Next, the  $\nu_{11}$  mode is observed around  $1,435 \text{ cm}^{-1}$  at 6 GPa. The  $\nu_{11}$  is fitted with three components from 6 to 8 GPa which we refer to as  $\nu_{11}(1)$ ,  $\nu_{11}(2)$ , and  $\nu_{11}(3)$ , respectively, in agreement with the previous study up to 8 GPa [3]. By 8 GPa, a fourth component becomes visible,

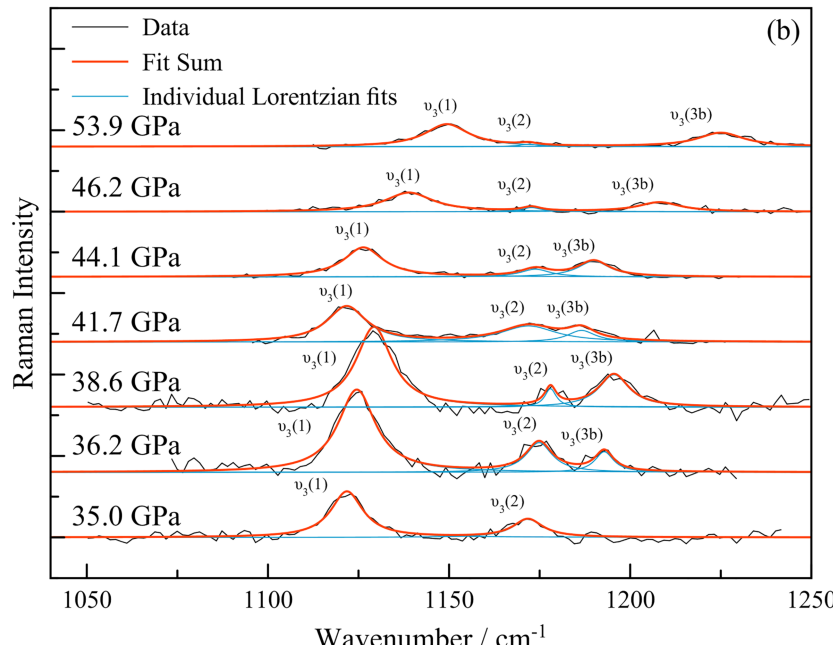
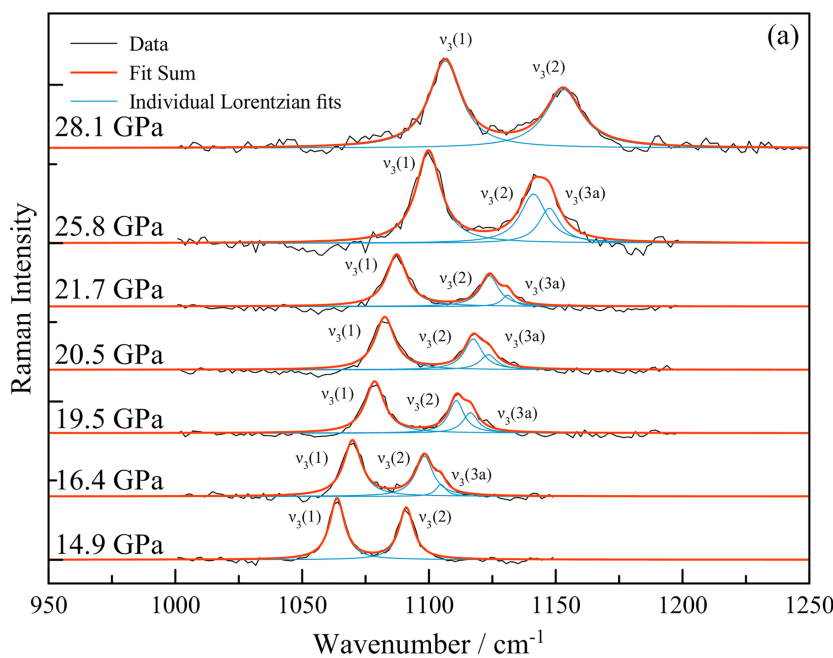


**FIGURE 1** (a) Raman spectra taken at pressures where the  $\nu_3(3a)$  component was observed. The spectra are shown with Lorentzian fits after background subtraction. (b) Example Raman spectra at various pressures within the pressure region of the splitting and subsequent disappearance of the  $\nu_3(2)$  component and growth of the  $\nu_3(3b)$  component. Spectra are shown with Lorentzian fits after background subtraction. The 54-GPa Raman spectrum is the final spectrum where  $\nu_3(2)$  could still be measured [Colour figure can be viewed at [wileyonlinelibrary.com](http://wileyonlinelibrary.com)]

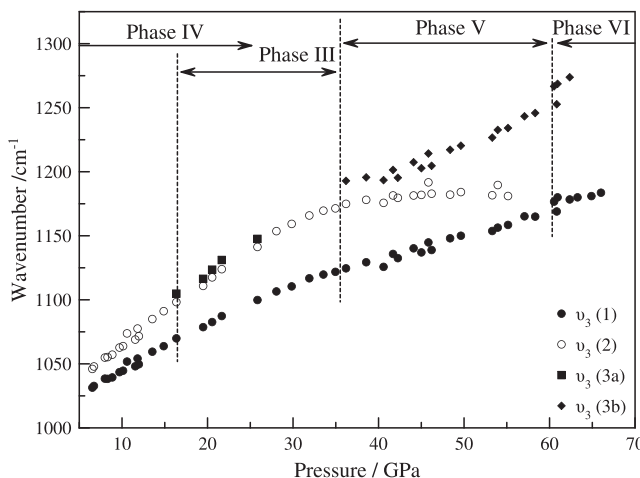


**FIGURE 2** Raman peak position as a function of pressure for the component peaks of the  $\nu_3$  Raman-active mode. Both splittings of the  $\nu_3(2)$  component are visible, around 20 and 40 GPa. The sudden change in gradient of the  $\nu_3(2)$  peak position/pressure function is visible past 30 GPa. Discontinuity can be noted in both  $\nu_3(1)$  and  $\nu_3(3b)$  past 60 GPa. The discontinuity of  $\nu_3(3b)$  takes place only shortly before its disappearance from measurement at 64 GPa

referred to as  $\nu_{11}(4)$ , splitting off from the highest wavenumber component. Figure 3a shows the spectra of this splitting.

At 20 GPa, the first component of  $\nu_{11}$  merges into the second and becomes no longer measurable (Figure 3b). The component peaks of  $\nu_{11}$  increase roughly linearly in wavenumber against pressure throughout, bar two discontinuous jumps located after 60 GPa. These are visible in Figure 4. Following the 60 GPa discontinuity, the  $\nu_{11}(2)$  component degrades and becomes immeasurable by 66 GPa as shown in Figure S4.

The remaining components of the  $\nu_3$  and  $\nu_{11}$  modes cannot be found at pressures of 75 GPa or above and thus must, at some point between 67 and 75 GPa, become immeasurable.

The final group of peaks consists of several overlapping peaks at  $\sim 3,000 \text{ cm}^{-1}$ . Using the nomenclature established in our earlier study of the liquid state [2], these are the  $(2\nu_8, 2\nu_{11})$  CH<sub>3</sub> deformation mode,  $\nu_5$ ,  $\nu_1$ , and  $\nu_{10}$  C-H stretching modes. We observe that upon crystallization, the  $\nu_5$  disappears and the  $\nu_{10}$  splits into two components. Thus, although both the liquid and the solid Raman spectra contain four components, they do not correspond to the same peaks. This observation is in agreement with Shimizu et al. [3]. A figure is provided in the supporting information comparing the fit in the solid state when the group is fitted with three and four components. Additionally, we have refitted our data from Proctor et al. [2] collected close to crystallization in

both the liquid and the solid states to illustrate the relation between the liquid and solid state peak assignments. This is also shown in a figure in the supporting information.

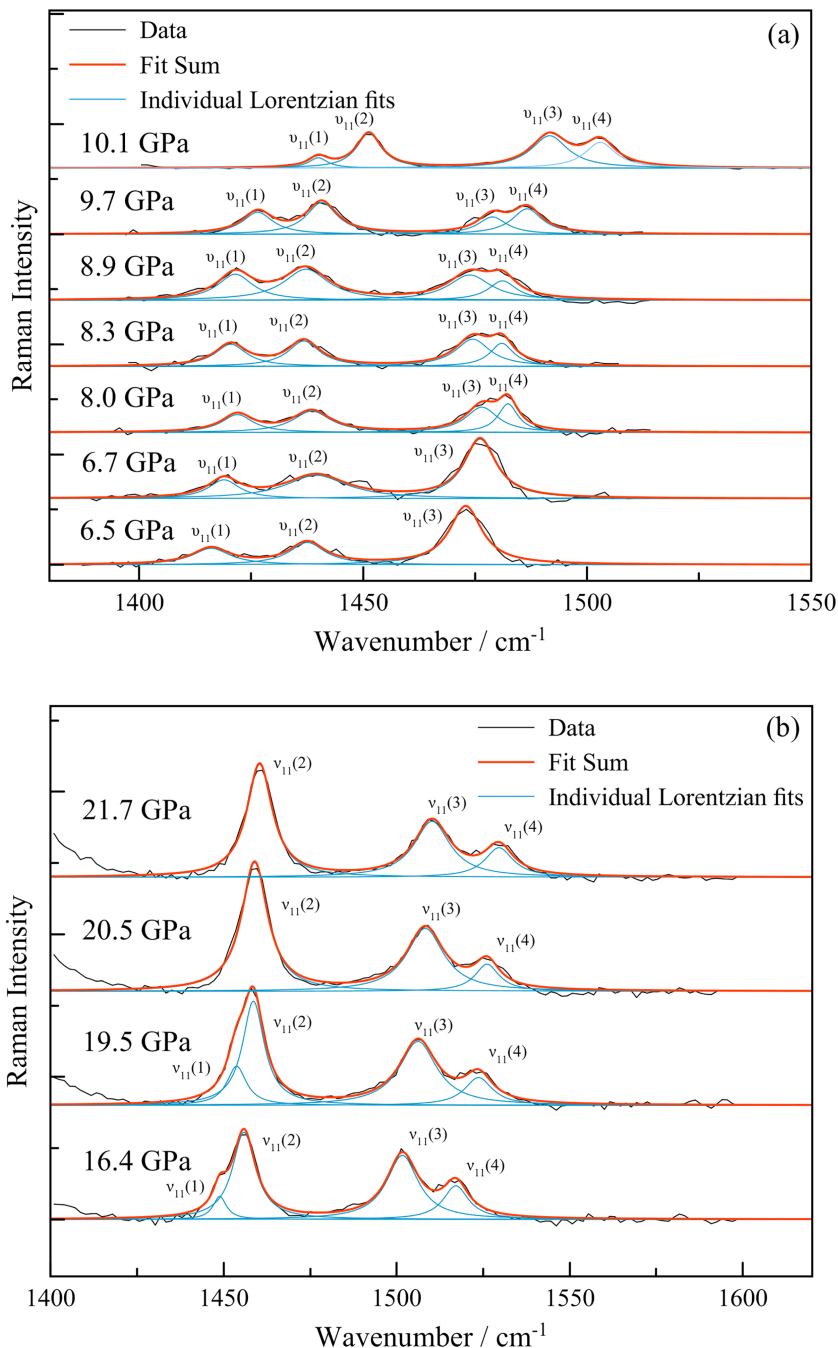
At higher pressure, all four peaks change discontinuously in wavenumber against pressure after passing 60 GPa; however, neither experiences any discontinuity or changes in peak composition beyond that throughout the data from 6 to 120 GPa. A full view of the peak progression of these modes is also given in the supporting information, along with the highest pressure spectrum at which each peak is observed where this is not shown elsewhere.

## 4 | DISCUSSION

In our earlier study of liquid ethane [2], we observed that our Raman spectra collected immediately upon crystallization at 2.5 GPa were similar to those presented in Shimizu et al. [3], but substantially different from those measured from Phase II at low temperature at 0.1 MPa [17]. We therefore attributed these spectra to Phase IV rather than Phase II. Following the more detailed study presented here, this remains our view.

At higher pressures, we suggest that there is strong evidence of three phase transitions taking place within our study. The concurrence of a temporary splitting of the  $\nu_3$  mode's second component (Figure 1) with the first component of the  $\nu_{11}$  mode becoming no longer measurable at 16–20 GPa (Figure 3b) is our first candidate for the location of a phase transition. We propose that this is the location of the Phase IV to Phase III transition, as observed by Goncharov et al. [5] at 18 GPa, not at 3.5 GPa as claimed in Shimizu et al. [3]. We do observe the gradual splitting of the  $\nu_{11}(3)$  component creating a subsequent  $\nu_{11}(4)$  component prior to around 8 GPa, similarly to Shimizu et al. [3], but we do not consider it to be evidence for a phase transition. We instead suggest that both peaks were present from crystallization at 2.5 GPa but inhabited the same wavenumber position then gradually diverging around 8 GPa, as we did not observe any discontinuities or effects on any other mode components as we have with the three transitions we suggest below. Given that Phase IV has two molecules in the primitive unit cell [4], Davydov splitting is an obvious candidate to explain the splitting in the  $\nu_3$  mode commencing immediately upon crystallization and shown both here and in Shimizu et al. [3]. Because the Davydov splitting is due to the interaction between the two molecules comprising the unit cell, it is to be expected that the magnitude of the splitting increases with density increase as observed here and also in other systems [18].

**FIGURE 3** (a) Raman spectra of the  $\nu_{11}$  mode showing the splitting of the  $\nu_{11}(3)$  mode and formation of a  $\nu_{11}(4)$  mode. The  $\nu_{11}(4)$  mode remains present in measurements until past 67 GPa. (b) Raman spectra of the  $\nu_{11}$  mode taken in the pressure region where  $\nu_{11}(1)$  merges with  $\nu_{11}(2)$ . The  $\nu_{11}(1)$  mode is not observed in our data from this point on. These figures show the Lorentzian fits after background subtraction [Colour figure can be viewed at [wileyonlinelibrary.com](http://wileyonlinelibrary.com)]



However, we also observe in our data the phase transition causing a temporary splitting of the  $\nu_3(2)$  component from 16 to 25 GPa as seen in Figure 1, implying a co-existence of phases IV and III from 16 to 25 GPa. As shown in Figure 2, the new component appearing at 16 GPa ( $\nu_3(3a)$ ) appears to line up the best with the continuation of the  $\nu_3(2)$  component beyond 25 GPa.

The second suggested phase transition begins at 35 GPa, which we will denote as the Phase III to Phase V transition. Within this region, we note that the plateauing of  $\nu_3(2)$  component at 35 GPa (Figure 2) and the degradation of the  $\nu_3(2)$  component are concurrent to

the growth of the  $\nu_3(3b)$  component beginning at ~35 GPa (Figure 1b). As previously discussed, we suggest that the observed  $\nu_3(3b)$  component that replaces the  $\nu_3(2)$  component is the same component as found splitting off of the  $\nu_3(2)$  component at 16 GPa (Figure 1).

The third phase transition takes place at ~60 GPa, which we will denote as the Phase V to Phase VI transition. The first evidence is the large discontinuous wavenumber against pressure jump found in almost all measured peaks. Following this, by 64 GPa, the  $\nu_3$  mode has reduced to one component and the  $\nu_{11}$  mode has reduced to two components. However, the reduction of

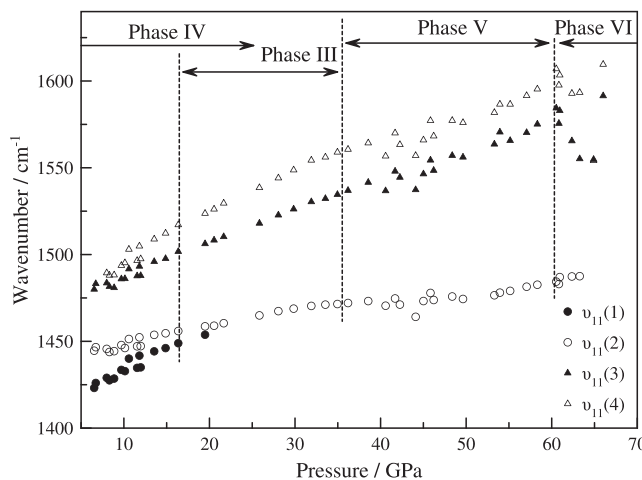


**FIGURE 4** Raman peak position as a function of pressure for the  $\nu_{11}$  mode components. The splitting of the  $\nu_{11}(3)$  component is visible around 7 GPa. The merging of the  $\nu_{11}(1)$  component into the  $\nu_{11}(2)$  component can be seen around 20 GPa. Discontinuities can be seen in  $\nu_{11}(2)$  and  $\nu_{11}(3)$  at around 62 GPa. The 62 GPa discontinuity is much more visible in the  $\nu_{11}(3)$  and  $\nu_{11}(4)$  mode

the  $\nu_{11}$  mode to two components can alternately be explained by the disappearing component seeming to merge with the diamond Raman peak and could in fact still be there even if unmeasurable.

At high pressures, we do not believe that the disappearance of the remaining components of the  $\nu_3$  and  $\nu_{11}$  modes entirely from measurement between 67 to 75 GPa constitutes evidence for a further phase transition. It could be caused by a continuation of this transition, or the modes could still exist but become too weak to measure. At such extreme pressures, solids are generally able to support significant static shear stress, and in the absence of any other effects, this generally causes the observed intensity of Raman modes to decrease.

We see no evidence of decomposition of our sample taking place. The ethane sample remained transparent and of the same shade throughout pressure testing and the intense hydrogen vibron at  $\sim 4,000 \text{ cm}^{-1}$  was never observed within our 120-GPa pressure limit. We note, however, that due to its small molecular size, hydrogen can diffuse out of the DAC very easily at extreme pressures.

Our first observed phase transition (that from Phase IV to Phase III commencing at 16 GPa) is in agreement with available EOS data [5]. However, Goncharov et al. [5] go on to state that no further phase transitions were observed up to the highest pressure reached in the study (120 GPa). We have examined the EOS data to discern the degree to which it is consistent with our hypothesis that further phase transitions are present. Due to the

small number of  $P,V$  data points above the Phase IV to Phase III transition at 16 GPa in Goncharov et al. [5] (13  $P,V$  measurements), the fitting of an EOS with a large number of adjustable parameters cannot be justified. We have fitted all 13 data points with a single Murnaghan EOS [19] with four adjustable parameters ( $K_0, K'_0, P_0, V_0$ ). In this case, we observe that the data at 60 GPa and above would be fitted better by an EOS with a lower bulk modulus. The fit quality is significantly improved by fitting two separate Murnaghan EOS, one to the data up to 60 GPa and one to the data at 60 GPa and above. This improvement is not due to an increase in the number of adjustable parameters in the EOS fit: in this case, we fixed  $P_0, V_0$  at their values for the lowest pressure data point in each fit so the number of adjustable parameters remained at 4 ( $K_0, K'_0$  for both EOS). These fits are shown in the supporting information. Probably, the fit could be improved further by fitting three separate EOS, but this is not possible without the number of adjustable parameters in the EOS becoming unacceptably large given the small number of data points.

## 5 | CONCLUSIONS

We have reported the Raman spectra of ethane at pressures up to 120 GPa at 300 K. We have observed activity in both  $\nu_3$  and  $\nu_{11}$  Raman active modes around 16–20 GPa and at  $\sim 35$  GPa in the form of component splitting and merging, discontinuity in the peak position function, and degradation of peak intensity to the point of immeasurability. We have also observed discontinuity in mode components past 60 GPa followed by the disappearance of components of both  $\nu_3$  and  $\nu_{11}$  modes. We have suggested that these three regions of activity represent phase transitions within our ethane sample. The first of these suggested transitions at 20 GPa backs up a previously suggested region for the Phase IV to Phase III ethane transition [5]. We have not observed any signs of the ethane molecule decomposing. If this took place, we would expect visually observable changes to the ethane sample and for the hydrogen vibron to be observable within our spectra. Neither of these was observed.

The extent to which our observations are consistent with the available diffraction is not clear because, from the published data (19  $P,V$  EOS points), the degree to which the structure is constrained by the need to fit to the observed diffraction data is not known. Resolving this matter would require a diffraction study outlining the structural refinement procedure in more detail. The raw diffraction data should be shown as well as the simulated diffraction patterns obtained through the structural refinement procedure. Due to the large amount of

hydrogen in ethane, this should ideally be conducted using neutron as well as x-ray diffraction.

## ACKNOWLEDGEMENTS

We would like to thank the anonymous reviewers for useful suggestions that have significantly improved the manuscript.

## ORCID

John E. Proctor  <https://orcid.org/0000-0003-3639-8295>

## REFERENCES

- [1] D. G. Friend, H. Ingham, J. F. Ely, *J. Phys. Chem. Ref. Data* **1991**, *20*, 275.
- [2] J. E. Proctor, M. Bailey, I. Morrison, M. A. Hakeem, I. F. Crowe, *J. Phys. Chem. B* **2018**, *122*, 10172.
- [3] H. Shimizu, I. Shimazaki, S. Sasaki, *Jpn. J. Appl. Phys.* **1989**, *28*, 1632.
- [4] M. Podsiadlo, A. Olejniczak, A. Katrusiak, *Cryst. Growth Des.* **2017**, *17*, 228.
- [5] A. Goncharov, E. Stavrou, S. Lobanov, A. Oganov, V. Roisen, A. Chanyshhev, K. Litasov, Z. Konopkova, K. Zhuravlev, V. Prakapenka, A. *Acta Crystallogr.* **2014**, *A70*, C757 (*conference abstract*). *Extended abstract* available at: <https://pdfs.semanticscholar.org/1dcb/928e0e4333b037effcd2da2dc95cc6c7ca8e.pdf>
- [6] A. Zerr, G. Sergiou, R. Boehler, M. Ross, *High Press. Res.* **2006**, *26*, 23.
- [7] J. D. Kemp, K. S. Pitzer, *J. Am. Chem. Soc.* **1937**, *59* (2), 276.
- [8] K. S. Noll, R. F. Knacke, A. T. Tokunaga, J. H. Lacy, S. Beck, E. Serabyn, *Icarus* **1985**, *65*, 257.
- [9] W. B. Hubbard, *Science* **1997**, *275*, 1279.
- [10] J. Bishop, S. K. Atreya, F. Herbert, P. Romani, *Icarus* **1990**, *88*, 448.
- [11] M. E. Summers, D. F. Strobel, *Astrophys. J.* **1989**, *364*, 495.
- [12] L. Van Der Putten, J. A. Schouten, N. J. Trappeniers, *Phys. B* **1986**, *144*, 215.
- [13] G. J. H. Van Nes, A. Vos, *Acta Crystallogr. B* **1978**, *34*, 1947.
- [14] A. Dewaele, M. Torrent, P. Loubeyre, M. Mezouar, *Phys. Rev. B* **2008**, *78*, 104102.
- [15] Y. Akahama, H. Kawamura, *J. Appl. Phys.* **2006**, *100*, 043516.
- [16] M. G. Wisnosky, D. F. Eggers, *J. Chem. Phys.* **1983**, *79*, 3505.
- [17] M. G. Wisnosky, D. F. Eggers, L. R. Fredrickson, J. C. Decius, *J. Chem. Phys.* **1983**, *79*, 3513.
- [18] R. Ouillon, J.-P. Pinan-Lucarré, B. Canny, P. Pruzan, P. Ranson, J. Raman, *Spectrosc.* **2008**, *39*, 354.
- [19] F. D. Murnaghan, *PNAS* **1944**, *30* (9), 244.
- [20] J. Romanko, T. Feldman and H.L. Welsh, *Can. J. Phys.* **1955**, *33*(10), 588.

## SUPPORTING INFORMATION

Additional supporting information may be found online in the Supporting Information section at the end of this article.

**How to cite this article:** Read LQ, Spender JE, Proctor JE. Raman spectroscopy of ethane ( $C_2H_6$ ) to 120 GPa at 300 K. *J Raman Spectrosc.* 2020;1–7. <https://doi.org/10.1002/jrs.5971>